

Article

Efficacy Evaluation of *Chlorella pyrenoidosa* Extracts on Cytotoxicity Induced by Atmospheric Particulate Matter 2.5 Exposure Using Skin Cell Lines and Zebrafish Models

Xiang Wang ¹, Xin Li ², Xufeng Jiang ³, Fengwei Xiang ⁴, Yuanliang Lai ⁴ and Guanggang Xiang ^{4,*}

¹ Shanghai Key Laboratory of Chemical Biology, School of Pharmacy, East China University of Science and Technology, Shanghai 200237, China

² School of Energy Power and Mechanical Engineering, North China Electric Power University, Beijing 102206, China

³ Singapore Ugel Cosmetics Pte. Ltd., Singapore 349561, Singapore

⁴ Shanghai Jiayu Bio-Technology Co., Ltd., Shanghai 201600, China

* Correspondence: xgg@whysbio.com

Abstract: The invention and use of chelating purification products directed at atmospheric particulate matter 2.5 (PM_{2.5}) are beneficial in preventing cytotoxicity and bodily harm. However, natural plant active compounds that minimize the adverse effect of PM_{2.5} are rarely reported. *Chlorella pyrenoidosa* extracts (CPEs), a nutritional supplement derived from *Chlorella vulgaris*, have been shown to have antioxidant and anti-inflammatory effects. Here, we discovered that CPEs extracted with crushing cell extraction technology can attenuate the negative impacts of PM_{2.5}. Furthermore, CPE intervention can protect against DNA damage and unstable genomic structure due to PM_{2.5} exposure. Moreover, CPE intervention restored mRNA and protein expression of the DNA misincorporation repair mechanism gene, nudix hydrolase 1 (*NUDT1*), and 8-oxoguanine DNA glycosylase (*OGG1*). In vivo damage protection experiments revealed that CPEs reduced PM_{2.5}-induced hepatotoxicity of zebrafish larvae and effectively prevented the death of adult zebrafish exposed to PM_{2.5}. Briefly, CPEs can attenuate cytotoxicity, resist DNA damage, relieve PM_{2.5}-induced hepatotoxicity, and improve cell purification activity, making them ideal for use as a protective factor or functional ingredient in the cosmetics and health food industries.

Keywords: *Chlorella pyrenoidosa* extracts; atmospheric particulate matter 2.5; cytotoxicity; skin cell; zebrafish



Citation: Wang, X.; Li, X.; Jiang, X.; Xiang, F.; Lai, Y.; Xiang, G. Efficacy Evaluation of *Chlorella pyrenoidosa* Extracts on Cytotoxicity Induced by Atmospheric Particulate Matter 2.5 Exposure Using Skin Cell Lines and Zebrafish Models. *Cosmetics* **2023**, *10*, 63. <https://doi.org/10.3390/cosmetics10020063>

Academic Editor: Piet van Erp

Received: 7 March 2023

Revised: 1 April 2023

Accepted: 10 April 2023

Published: 12 April 2023



Copyright: © 2023 by the authors. Licensee MDPI, Basel, Switzerland. This article is an open access article distributed under the terms and conditions of the Creative Commons Attribution (CC BY) license (<https://creativecommons.org/licenses/by/4.0/>).

1. Introduction

Air pollutants are the inevitable types of pollutants in our daily life and study, which affect personal health and promote the occurrence of acute and chronic diseases. Plant active extracts, with the functional characteristics of pure natural, green and healthy, have been widely used in the research and practical application of anti-air pollutant damage. Studies have shown that plant extracts can alleviate many health problems caused by air pollutants, such as alleviating corneal inflammation, reducing lung injury, improving the antioxidant capacity of the body, repairing skin barriers, and so on [1–7]. The freshwater microalga *Chlorella vulgaris* (*C. vulgaris*) is a green spherical single-celled organism (2–10 µm in diameter) belonging to the phylum *Chlorophyta* [8]. *C. vulgaris* has been widely used as a food supplement and is credited with high antioxidant and therapeutic properties, making it one of the 21st-century human need green nutrition source health foods listed by the United Nations Food and Agriculture Organization (FAO) [9,10]. *Chlorella* extract exhibits immunological [11], blood glucose-lowering [12], anti-tumor [13], and anti-oxidative effects [14]. Therefore, using *chlorella* extracts as a food supplement or active additive may be a natural, economical and safe strategy to counteract the factors that cause cytotoxicity, DNA damage, apoptosis, such as reactive oxygen species (ROS) and inflammatory factors.

Atmospheric particulate matter 2.5 (PM_{2.5}, which refers to airborne particles with a direct diameter less than 2.5 μm) is a probable source of hazy weather and related respiratory diseases, and it gravely threatens health and quality of life [15]. Numerous studies have shown that exposure to PM_{2.5} can harm multiple body systems, leading to illnesses associated with the respiratory system [16], nervous system [17], immune system, and reproductive system [18]. Subsequent studies have revealed that these diseases are brought on by PM_{2.5} damage to the cells that make up the organs. Skin diseases such as allergic dermatitis, eczema, acne, and skin aging are all linked to environmental PM_{2.5} pollution. Application of contemporary biological technology to discover therapies against the negative effects of PM_{2.5} has become a critical requirement for today's social development, particularly in improving living standards and paying attention to the wellbeing of people.

PM_{2.5} is characterized by complex and diverse components, and it can disrupt the normal physiological state and biological function of cells in a variety of ways. Nonetheless, multi-channel intervention can minimize the harmful impact of PM_{2.5}. In the present investigation, we employed two self-developed patented technologies for atmospheric PM_{2.5} collection (CN106442250A) [19], CPEs enzymatic and crushing extraction (CN106236623A) [20] to evaluate the intervention effect of CPEs against PM_{2.5} exposure in cells and zebrafish models. Furthermore, we investigated the bioactivity of CPEs and their potential to resist the cytotoxic effects of PM_{2.5} using heavy metal chelation, cell viability, and cell proliferation assays. The genetic protective effect and potential protective mechanism of CPEs were investigated using comet electrophoresis and γH2A staining. The purifying effect of CPEs on toxin accumulation was verified by a Zebrafish experiment.

Together, these pre-mechanistic studies using cell and animal models have illustrated the cell purification capacity of CPEs against PM_{2.5} that could provide a basis for food function research and application prospects in the cosmetics and health industries to combat PM_{2.5}.

2. Materials and Methods

2.1. Chemicals and Reagents

Dimethylsulfoxide (DMSO), low melting agarose, 4',6-diamidino-2-phenylindole (DAPI), normal melting agarose, 3-(4,5-dimethylthiazol-2-yl)-2,5-diphenyltetrazolium bromide (MTT), Tween 20, and paraformaldehyde were obtained from Sigma-Aldrich (St. Louis, MO, USA). FBS, RPMI cell medium, and penicillin–streptomycin were obtained from Gibco Life Technologies (Waltham, MA, USA). Triton X-100, non-fat powdered milk, Tris-base, glycine, sodium dodecyl sulfate (SDS), and ethylene diaminetetra acetic acid (EDTA) were obtained from Sangon Biotech Co., Ltd. (Shanghai, China). Trizol reagent was obtained from Tiangen Biotech (Beijing, China). Bicinchoninic acid (BCA) Protein Assay Kit, Reverse Transcription Kit, and SYBR green qPCR Master Mix were purchased from YEASEN (Shanghai, China). Primary antibodies (*NUDT1*, *OGG1*, β-actin) were obtained from Abcam (Cambridge, Cambs, UK). HRP-conjugated secondary antibodies were purchased from Proteintech (Rosemont, IL, USA). Polyvinylidene fluoride (PVDF) was purchased from Millipore Corp (Merk, Darmstadt, Germany). Titanchem Co. Ltd. (Shanghai, China) supplied other common chemicals.

2.2. *Chlorella vulgaris* Culture and Extract Preparation

Chlorella vulgaris was obtained from the East China University of Science and Technology (Shanghai, China) and cultured in Bold's basal media with a 12/12 h light–dark cycle. Figure 1 depicts the extraction procedure with the patent material [20]. Briefly, the cells were suspended in distilled water at 10% (*w/v*) concentration and maintained at 45–55 °C. Cellulase and pectinase were introduced at 1.2% of volume fraction for 1.5 h of hydrolyzation and crushing extraction for 2 min every 15 min. The extractives were then filtered and blended with 10% glycerol (*v/v*) to eliminate impurities and kept for 12 h at −4 °C. Subsequently, the supernatants were filtered and concentrated to 20–30% of liquid

weight using a nanofiltration membrane, sterilized and homogenized (≤ 45 °C, 200 MP), and lyophilized to yield active ingredients of *C. vulgaris*, dubbed *chlorella* purification effector molecules. The CPEs were dissolved in phosphate-buffered saline (PBS) or RPMI cell medium to achieve the desired concentration for subsequent use.

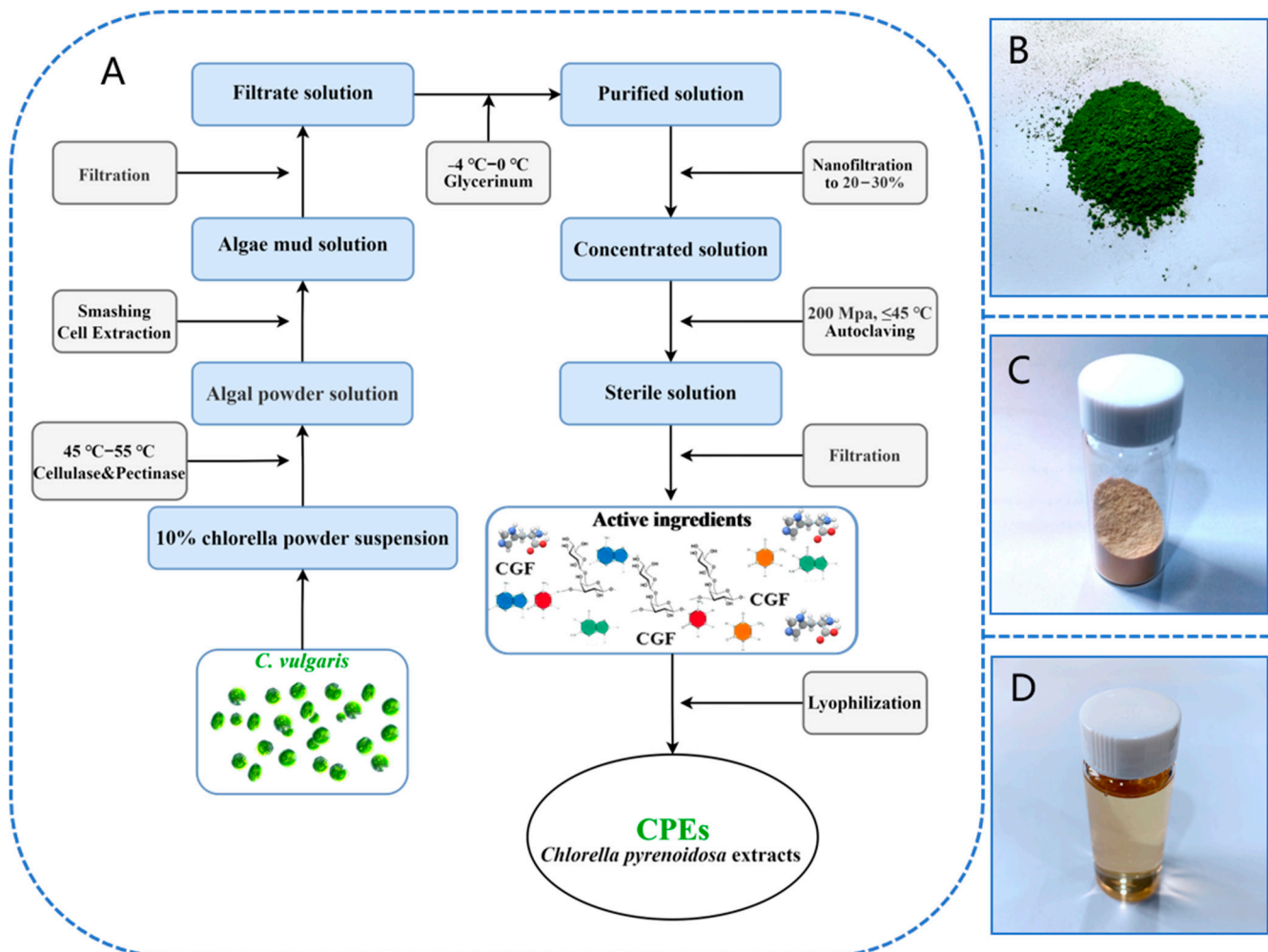


Figure 1. The extraction process of CPEs (A) and images of *Chlorella pyrenoidosa* (B) and its ex-tract (C) lyophilized powder; (D) aqueous solution.

2.3. Preparation of Atmospheric PM_{2.5}

The extract of PM_{2.5} was prepared in a continuous collection in central Shanghai (Xujiahui region) from 15 December 2019 to 15 January 2020 using our patented device (Figure 2A,B) for more than 20 h per day [21] and pumping to maintain a constant flow rate (1.13 ± 0.113 m³ min⁻¹). The filter membrane was removed after sampling and immersed in a suitable volume of ultrapure water for 20 min of ultrasonic oscillation; this was repeated 3 times. The resultant lotion was placed in a -80 °C refrigerator for 1–2 h, dried in a cryogenic freeze dryer to obtain PM_{2.5} dry powder, and stored in a -20 °C refrigerator for later use. The PM_{2.5} dry powder was mixed with PBS to make a 1 mg mL⁻¹ PM_{2.5} reserve solution, which was stored in a refrigerator at 4 °C for no more than one week. The PM_{2.5} suspension was ultrasonically mixed for 10 min and diluted in RPMI medium to required concentrations (50, 100, 200, 400, 800, 1600 µg mL⁻¹).

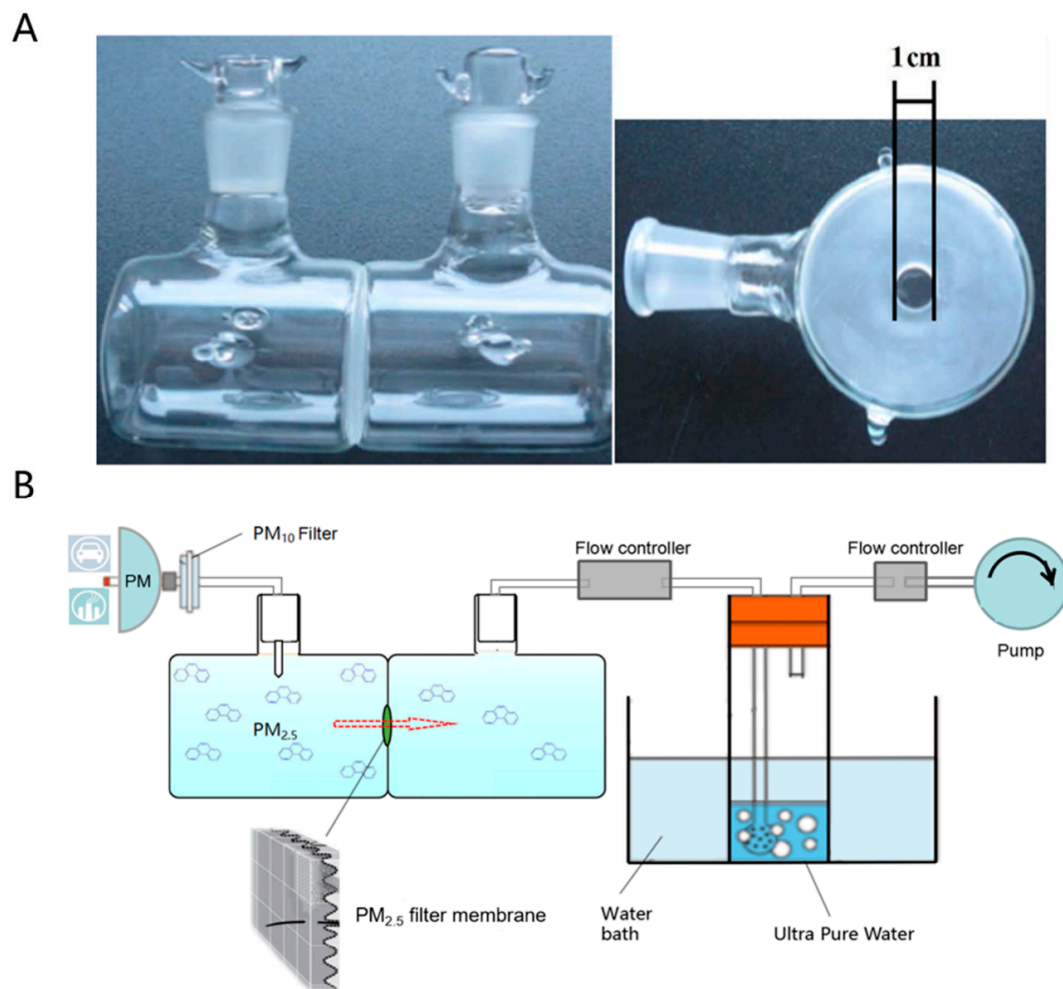


Figure 2. The collection device and process of atmospheric PM_{2.5}. (A) The structure of PM_{2.5} extraction device. (B) PM_{2.5} extracts manufacturing process schematic diagram.

2.4. Cell Culture

Human dermal fibroblasts and epidermal HaCaT cells were used as skin test evaluation models and were maintained in RPMI medium supplemented with 10% fetal bovine serum (FBS) and penicillin–streptomycin at 5% CO₂ and 37 °C.

2.5. Copper Ion Chelating Activity

The metal chelating potential of the sample was examined using the approach outlined by [22]. Briefly, isochoric (20 µL) CPEs and copper ion solution (2.5 mM) were mixed in 200 µL NaAc buffer (50 mM, pH 6.0) and left to stand for 30 min. This was followed by the addition of 5 µL pyrocatechol violet (20 mM, PV) and vigorous shaking. The color change was detected at 632 nm using an automated microplate reader (Multiskan Ex; Ani Lab Systems Ltd., Vantaa, Finland). The EDTA was used as a standard at 1 mg mL⁻¹.

2.6. Cell Viability

The MTT assay was used to assess cell viability under PM_{2.5} exposure [23]. Cells were seeded onto 96-well plates at a density of 5×10^4 cells/well⁻¹, allowed to adhere overnight, and then incubated for 24 h. Subsequently, MTT solution (5 mg mL⁻¹) was added to each well, and samples were incubated for an additional 4 h at 37 °C. The supernatants were then replaced with 100 µL DMSO. The optical density was measured at a test wavelength of 570 nm using an automated microplate reader (Multiskan Ex; Ani Lab Systems Ltd.,

Vantaa, Finland). The significant concentration of PM2.5 was determined using the MTT assay for subsequent experiments.

2.7. Cell Counting

The fibroblasts (at the logarithmic growth stage) were inoculated into 24-well plates to 60% confluence and treated for 12, 24, and 48 h, depending on the effective concentration of PM2.5 in the MTT assay. The cells were then digested with trypsin and suspended in PBS. Cells were counted using a hemocytometer.

2.8. Cell Cycle

Following 24 h treatment in 24-well plates, fibroblasts were washed twice with PBS after trypsinization (centrifugation for 5 min at $1000 \times g$, each time). Precooled 70% ethanol (dilute with distilled water) was gently mixed with cells and fixed at 4 °C for 1 h. The cells were centrifuged, washed twice, mixed with propidium iodide (PI), and then incubated at 37 °C for 30 min. Data were collected using flow cytometry (Beckman CytoFLEX LX, Pasadena, CA, USA), and Modfit LT software 5.0 was used to analyze cell cycles.

2.9. Cell Proliferation Ability

The 5-ethynyl-2'-deoxyuridine (EdU) assay [24]. Fibroblasts were cultured in 48-well plates to 60% confluence and treated for 24 h and then incubated with 50 μM EdU for 2 h. The cells were then fixed with 4% paraformaldehyde (PFA) for 30 min under ambient temperature, neutralized with 2 mg mL^{-1} glycine for 5 min, and permeabilized for 20 min on a shaking table with PBS containing 0.5% Triton X-100. The cells were supplemented with 1 \times Apollo staining solution, incubated for 30 min, washed three times in PBS containing 0.5% Triton X-100, and stained with 1 \times Hoechst 33342 solution. Finally, images were taken with a fluorescence microscope (Leica, DMI3000B, Wetzlar, Germany) and analyzed using Image J 1.51j8.

2.10. Alkaline Comet Assay

DNA damage was assessed using a single-cell gel electrophoresis (SCGE) assay in alkaline conditions (comet assay) [25]. Briefly, fibroblasts were treated for 24 h and harvested. Subsequently, a 30 μL cell sample (1×10^4 cells) was suspended in 110 μL of 1% molten low-melting-point agarose at 37 °C. The monosuspension was cast on a microscopic slide coated with a layer of 0.8% agarose. Images were captured with a fluorescence microscope (Olympus BX53, Tokyo, Japan) with a 515–560 nm filter and processed using CASP Lab (www.casp.of.pl).

2.11. Immunostaining and γH2AX Focus Quantification

The phosphorylation of histone γH2AX at Ser 139 (γH2AX) was analyzed as previously described [26]. Briefly, cells were seeded to 60% confluence in 24-well plates and treated for 24 h. Cells were then fixed in 4% paraformaldehyde for 15 min, washed with PBS, and permeabilized in 0.2% Triton X-100 for 20 min. Cells were blocked with goat serum for 1.5 h and incubated with a mouse monoclonal anti- γH2AX antibody (1:1000 dilution, Cell Signaling Technology, Inc., Danvers, MA, USA) for 2 h; this was followed by 1 h incubation with TRITC-conjugated goat anti-mouse secondary antibody (1:500 dilution, Cell Signaling Technology, Inc., Danvers, MA, USA). The cells were incubated with DAPI at room temperature for an additional 5 min to achieve nuclear staining. The cells were then mounted in an antifade medium, and images were captured with a fluorescence microscope (Olympus BX53, Japan). A threshold number of four H2AX foci per cell was selected as the optimal DNA damage assessment [27].

2.12. Zebrafish Toxicity and Protection Testing

Transgenic Tg (Apo14: GFP)-type adult and wild-type adult zebrafishes were provided by the Guangdong Laboratory Animals Monitoring Institute. Fifty larvae bred from Transgenic Tg (Apo14: GFP) type at the 3 dpf (days postfertilization, dpf) stage were immersed in 3–4 mL of solutions containing PM2.5 (100 $\mu\text{g mL}^{-1}$) or with CPEs (10 mg mL^{-1}) for 3 days. The larvae were developed under standard conditions. Following treatment, 25 zebrafish in each culture plate were visually examined and photographed using a fluorescence microscope (Nikon, Tokyo, Japan). Every 8–10 wild-type adult zebrafish were cultured in 500 mL filtered water for each group. One group was treated with PM2.5 (10 mg mL^{-1}), and another group was treated with additional CPEs (10 mg mL^{-1}) for intervention. The survival status of zebrafish in the two groups was monitored continuously for 10 min, and the number of dead and surviving zebrafish in each group was recorded to calculate survival rates. The experiment was performed in three independent replicates. All experiments complied with guidelines for the Animal Care Committee of East China University of Science and Technology (approval number #2006272).

2.13. Real-Time Quantitative RT-PCR

Total RNA was extracted using Trizol reagent (TIANGEN, Beijing, China), and RNA concentration was determined with a microplate reader (BioTek, Winooski, VT, USA). Total RNA (1000 ng) was reverse transcribed into cDNA using a reverse transcription kit following the manufacturer's protocol. Real-time qRT-PCR analysis was performed with an SYBR Green Kit on Applied Biosystems Real-Time PCR System (BIO-RAD CFX96, Hercules, CA, USA) with the following reaction conditions: 50 °C 2 min, 95 °C 10 min, 40 cycles for 95 °C 15 s, 60 °C 60 s. Data were analyzed using the $2^{-\Delta\Delta\text{Ct}}$ method. The primers are listed in Table 1.

Table 1. The primer sequences for qRT-PCR.

Gene	Forward (5'–3')	Reverse (5'–3')
NUDT1	GTCATGGACGTGCATGTCTT	GTGGAAACCAGTAGCTGTCGT
OGG1	ATGGGGCATCGTACTCTAGC	CTCCCTCCACCGGAAAGAT
β -actin	CATGTACGTTGCTATCCAGGC	CTCCTTAATGTCACGCACGAT

2.14. Western Blotting

Cells were lysed in RIPA buffer containing a protease inhibitor and scraped into an Eppendorf tube, where they were incubated for 5 min after each 20 s vortex, a total of 6 times. The entire procedure was performed on ice. Protein concentrations were measured using BCA protein quantification Kit. Proteins (approximately 20 μg) were separated using a 12.5% SDS-PAGE gel fast preparation kit (Epizyme, Shanghai, China) and transferred to Immobilon-P PVDF membranes (Millipore, Darmstadt, Germany). Membranes were blocked with 5% non-fat milk in Tris-buffered saline Tween 20 (TBST, TBS with 0.5% Tween 20) for 1.5 h at room temperature with gentle shaking, then incubated overnight at 4 °C with 1:1000 dilution antibodies (anti- γH2AX , anti-*OGG1*, anti-*NUDT1*, and anti- β -actin). The membranes were washed with TBST three times for 10 min each, followed by two hours of incubation with HRP- blocking buffer (5% non-fat milk in TBST)-diluted conjugated secondary antibodies 1:2000, and then washed three times with TBST for 10 min each. Finally, protein bands were visualized using ECL reagent (Tanon, Shanghai, China) and scanned by the Gel Imager System (Tanon, 4600SF, China). The grayscale value of protein bands was determined by Image J.

2.15. Statistical Analyses

Data were subjected to variance analysis (ANOVA) to compare treatment differences and interactions; statistical significances were assessed by a two-tailed Student's *t* test.

GraphPad Prism 8.0 software was used for the statistical analysis (* $p \leq 0.05$; ** $p \leq 0.01$). All experiments were performed in triplicates, and the results are expressed as mean \pm SD.

3. Results

3.1. Biological Activity of CPEs from *C. vulgaris* Extracts

The heavy metal chelating activity of CPEs served as a criterion for quality evaluation by spectrophotometry assay to assess the quality of CPEs extracted from *C. vulgaris* using the patented device (CN106236623A). The CPEs were revealed to function similarly to EDTA in competitively chelating copper ions, and the blue intensity was comparable to the PV and EDTA groups (Figure 3A). The CPEs chelated copper ions in a concentration-dependent manner, and significantly at 10 mg mL^{-1} , the copper ion chelating ratio of CPEs was 57.33% (Figure 3B). HaCaT cells were used to verify the chelating activity of CPEs for heavy metals in cells. Of note, CPEs (10 mg mL^{-1}) effectively restored cell viability loss caused by heavy metal ions in a medium enriched with $\text{K}_2\text{Cr}_2\text{O}_7$ ($10 \mu\text{M}$) and CdCl_2 ($20 \mu\text{M}$) over 24 h (Figure 3C,D). These findings suggested that *C. vulgaris*-derived CPE extracts have biological activity.

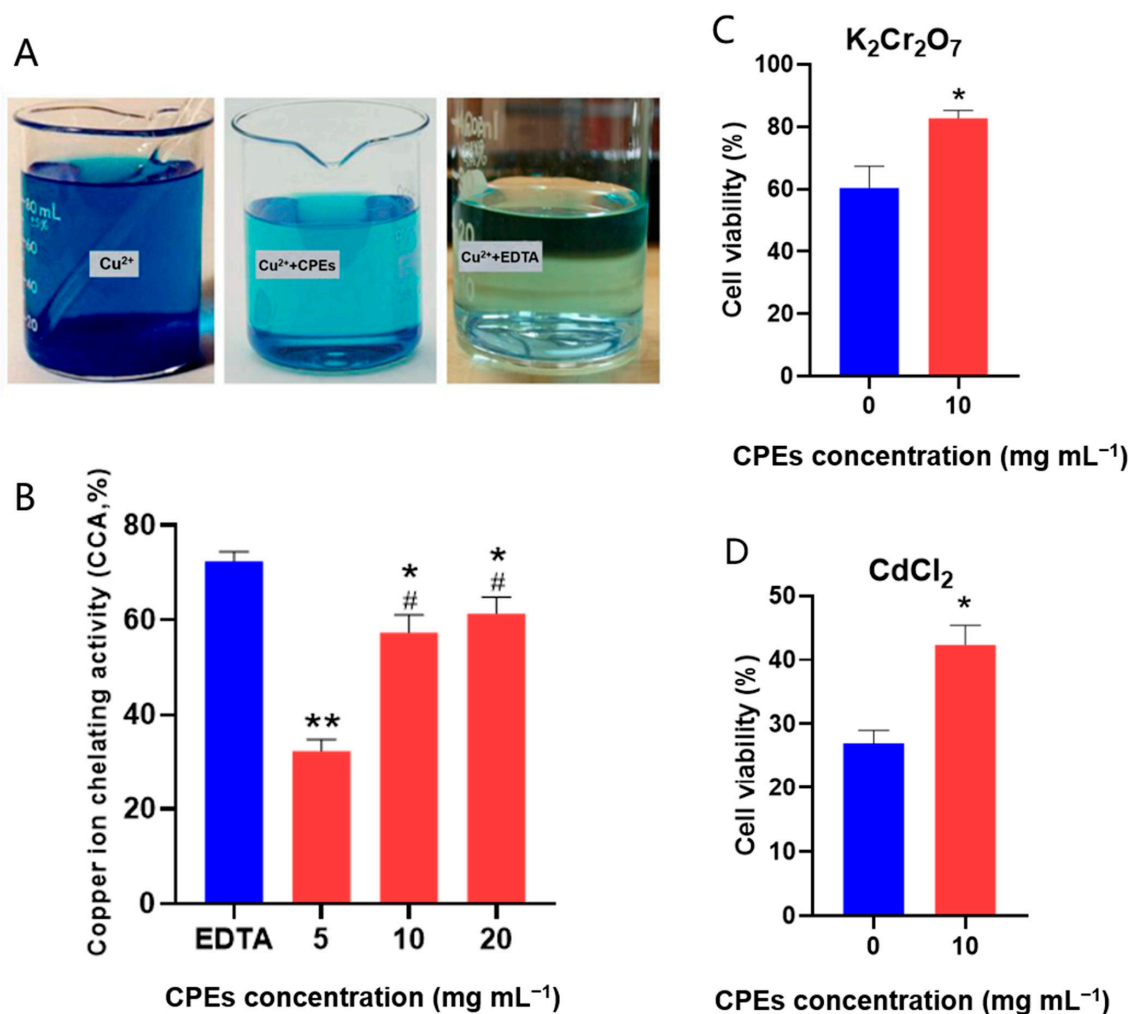


Figure 3. The activity identification of CPEs. (A,B) Copper ion chelating activities of the CPEs. Copper ion chelating activity of the CPEs at 5, 10, 20 mg mL^{-1} and EDTA at 1 mg mL^{-1} were detected at 632 nm. (C,D) Chromium ion and cadmium ion chelating activities of the CPEs in HaCaT cell. Cells were administrated with $\text{K}_2\text{Cr}_2\text{O}_7$ ($10 \mu\text{M}$) or CdCl_2 ($30 \mu\text{M}$) and then added to CPEs (10 mg mL^{-1}) for 24 h, and cell viability was tested by MTT assay. All results are expressed as mean \pm SD of three biological replicates. (B) * $p < 0.05$, ** $p < 0.01$ compared with MT; # $p < 0.05$ compared with CPEs (5 mg mL^{-1}); (C,D) * $p < 0.05$ compared with CPEs (0 mg mL^{-1}).

3.2. CPEs Resist PM2.5 Cytotoxicity and Maintain Cell Viability

To test the anti-cytotoxicity of CPEs, human skin fibroblasts were treated with gradient concentrations of PM2.5 (50, 100, 200, 400, 800, 1600 $\mu\text{g mL}^{-1}$) at different time points (12, 24, 48 h), and CPEs (10 mg mL^{-1}) were introduced into the medium as an intervention factor. Meanwhile, changes in cell morphology were noted, and cell viability was determined with the MTT assay. The data demonstrated that PM2.5 evoked a concentration-dependent decrease in fibroblast viability, with a significant decline at 100 $\mu\text{g mL}^{-1}$, but CPEs could counteract the toxic effect of PM2.5 and maintain cell viability (Figure 4A). Moreover, the cells took the shape of a wire drawing, and their proliferation ability decreased significantly following PM2.5 treatment. However, compared with the PM2.5 group, the CPEs had no toxic effect on cells and maintained their morphology and normal cell proliferation after 12, 24, and 48 h of treatment, which were comparable to the PBS group (Figure 4B). In addition, cell counting assay revealed that CPEs potentially restored the viability decrease in fibroblasts caused by PM2.5 toxicity (Figure 4C). These results demonstrated that CPEs can reduce the cytotoxicity induced by PM2.5 and maintain the fibroblasts' cell viability.

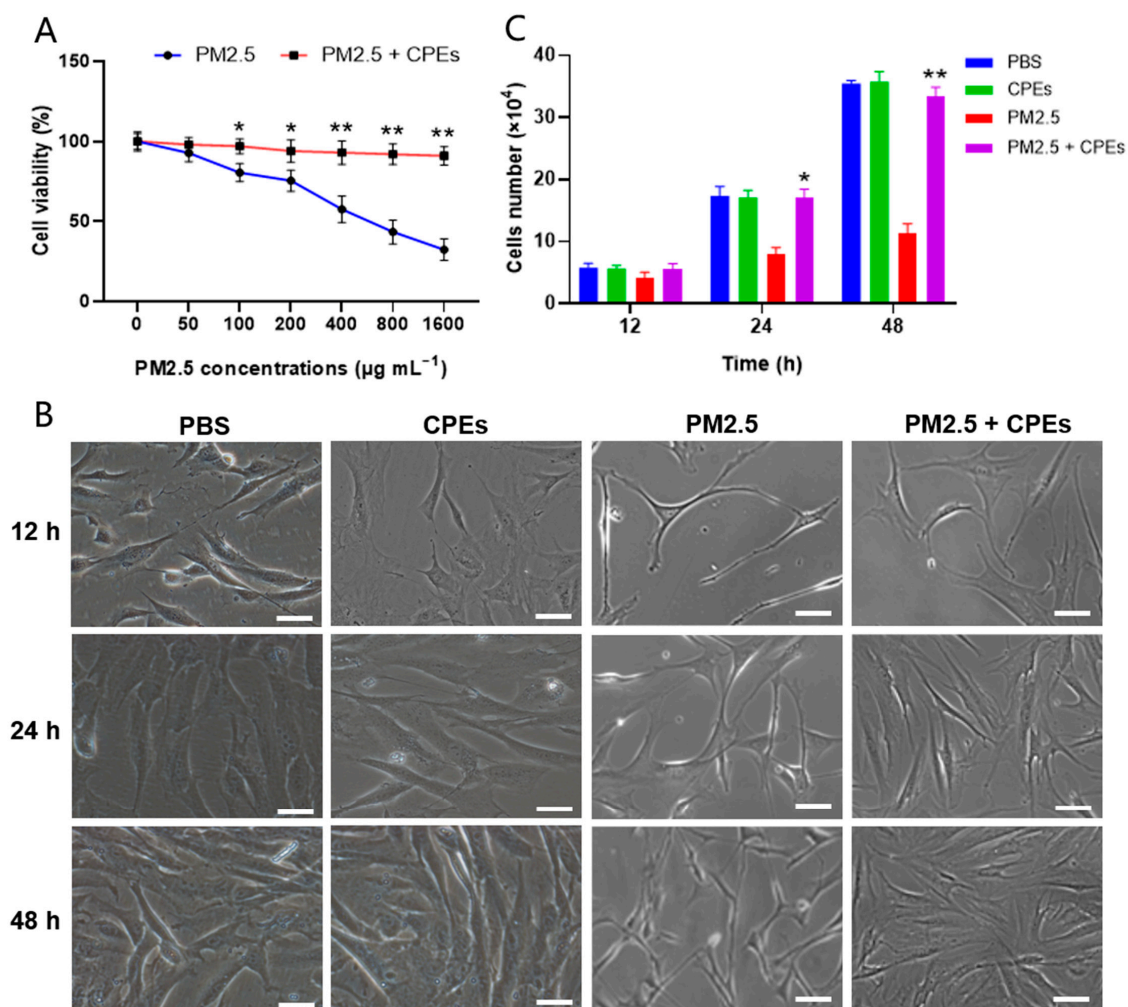


Figure 4. Cytotoxicity of PM2.5 on human skin fibroblasts and protective effect of CPEs in cell viability. (A) Fibroblasts were treated with increased concentrations of PM2.5 for 24 h, and CPEs (10 mg mL^{-1}) were added. (B) Changes in morphology of fibroblasts at 12, 24 and 48 h after addition of PM2.5 (100 $\mu\text{g mL}^{-1}$) or plus CPEs (scale bar: 50 μm). Cell viability was determined by MTT assay. (C) Cell numbers were counted after 12, 24, 48 h of treatment with PM2.5 or plus CPEs. All results are expressed as mean \pm SD of three biological replicates. * $p < 0.05$ and ** $p < 0.01$ compared with PM2.5.

3.3. CPEs Restore PM2.5-Induced Reduction in Cell Proliferation Ability

Considering that PM2.5 cytotoxicity influences cell proliferation, we further investigated the effect of PM2.5 on the cell cycle. Our analysis revealed a significant decrease in the proportion of S-phase cells in the PM2.5 group. These data suggested that PM2.5 treatment results in the S-phase arrest of fibroblasts, whereas CPE supplementation restores the number of S-phase cells (Figure 5A,B). Furthermore, we employed the EdU assay to assess cell proliferation ability under CPE treatment. Consistent with the flow cytometry assay results, the PM2.5 group had fewer EdU-positive cells (red) compared with the CPE group (Figure 5C). The proliferation rate, percent of EdU positive cells (red) in DAPI-positive cells (blue), calculated by Image J software, was significantly higher (up to 34.43%) in the CPE group than in the PM2.5 exposure group (down to 17.28%) (Figure 5D). Briefly, CPEs mitigated the effects of PM2.5 exposure by enhancing the normal proliferation ability of skin fibroblasts.

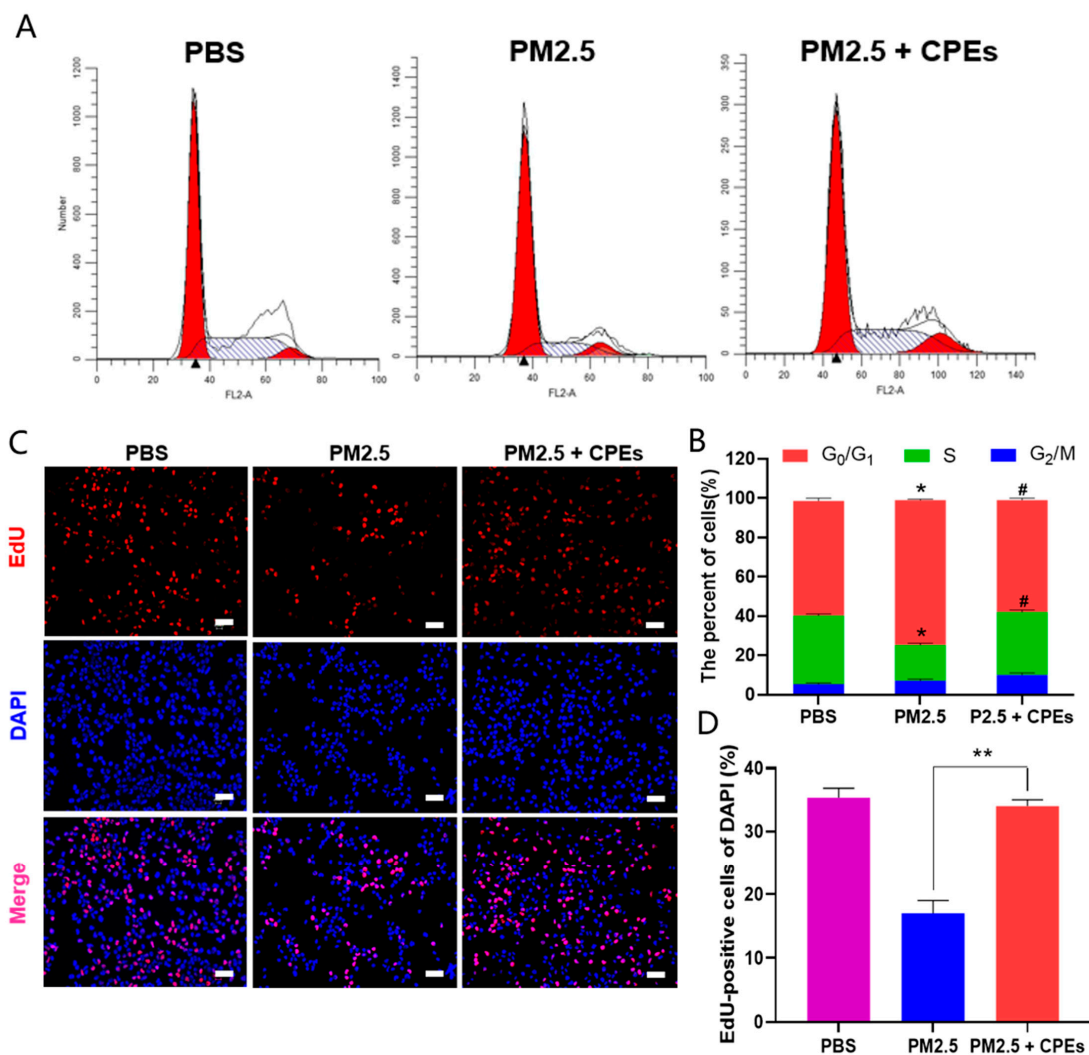


Figure 5. Effects of PM2.5 and CPEs on proliferation ability of fibroblasts. Cells were treated with PM2.5 ($100 \mu\text{g mL}^{-1}$) or plus CPEs (10 mg mL^{-1}) for 24 h. (A) Flow cytometry was used to analyze the changes in the cell cycle after PM2.5 or plus CPE treatment. (B) CPEs increased the proportion of S-phase cells resulting from PM2.5 treatment. (C) 5-ethynyl-2'-deoxyuridine staining (EdU, red) was used to indicate S-phase cells, and DAPI (blue) was used for nuclei staining (scale bar: $40 \mu\text{m}$). (D) Proliferation rate was significantly restored from the CPE-treated groups. All results are expressed as mean \pm SD of three biological replicates. (B) * $p < 0.05$ compared with PBS; # $p < 0.05$ compared with PM2.5. (D) ** $p < 0.01$ compared with PM2.5.

3.4. CPEs Prevent Human Skin Fibroblasts from PM2.5-Induced DNA Damage

Taking into account the protective roles of CPEs in cell viability and proliferation, we investigated the potential of CPEs to repair DNA damage for single- and double-strand breaks. The alkaline comet assay demonstrated the fragment migration caused by DNA single-strand break. The fluorescence intensity of DNA fragments was higher than that of the control, and PM2.5 impaired DNA single-strand structure, resulting in diffuse, broom-shaped comet-like tails (Figure 6A and Table 2). However, comet heads from the CPE group eventually recovered concentrated high-density DNA after 24 h, together with a smooth edge and intact nucleus, just like comet heads from the control group (Figure 6A). However, comet heads from the CPEs group gradually recovered concentrated high-density DNA after 24 h, accompanied by smooth margin and intact nuclei as in the control group (Figure 6A). The analysis revealed that CPEs lowered the comet-positive rate to 9% compared with 53% of PM2.5, which was close to 3.3% of the PBS control (Figure 6B). Figure 6C illustrates the immunofluorescent images of phosphorylation of histone H2AX in γ H2AX-stained human skin fibroblasts, which verifies the protective effect of CPEs on double-strand breaks. Human skin fibroblasts in the control group were characterized by few γ H2AX foci in the nuclei, and roughly 5% of cells had more than four foci. Furthermore, CPEs in the treatment groups decreased the percentage of γ H2AX-foci-positive cells associated with PM2.5-induced foci development (Figure 6C,D). Consistent with the results of the comet assay, CPEs demonstrated a favorable effect in preventing DNA damage in γ H2AX immunofluorescence assay. Notably, the γ H2AX positive rate dropped to 22.7% for CPE intervention in comparison to 82.3% under PM2.5 exposure (Figure 6D).

Table 2. The parameters of DNA damage in alkaline comet assays of fibroblasts with PM2.5 or plus CPEs treatment for 24 h. PBS-treatment was used as the negative control.

Treatment Group	Comet assay Parameters		
	Tail DNA (%)	Tail Length (μ m)	Tail Moment
PBS	2.31 \pm 0.45	2.62 \pm 0.22	0.12 \pm 0.12
CPEs	2.27 \pm 0.37	2.48 \pm 0.31	0.09 \pm 0.17
PM2.5	27.14 \pm 0.27	23.42 \pm 0.13	17.54 \pm 0.57
PM2.5 + CPEs	12.72 \pm 0.44	18.22 \pm 0.21	2.22 \pm 0.62

Nucleic acid damage repair is a cellular mechanism in response to DNA damage, mismatch, mutation, and other genotoxic effects. PM2.5 produces DNA damage in human skin fibroblasts; as such, we investigated the role of PM2.5 in the DNA damage repair pathway. Base excision repair (BER) is one of the primary DNA damage repair mechanisms, with *OGG1* and *NUDT1* acting as effector enzymes to remove damage marker 8-oxoG [28]. Therefore, qRT-PCR and Western blot assays were performed to verify the effect of PM2.5 on DNA damage repair and the protective effect of CPEs. The results showed that both mRNA and protein expression decreased following PM2.5 treatment and recovered to near-normal levels with CPEs, indicating that PM2.5 has a detrimental effect on the repair mechanism of DNA damage and that CPEs have a beneficial influence on this effect (Figure 6E–G). These data collectively demonstrate that CPEs have a great potential to maintain genomic integrity, protect DNA structure damage, and inhibit PM2.5-induced reduction of *NUDT1* and *OGG1*.

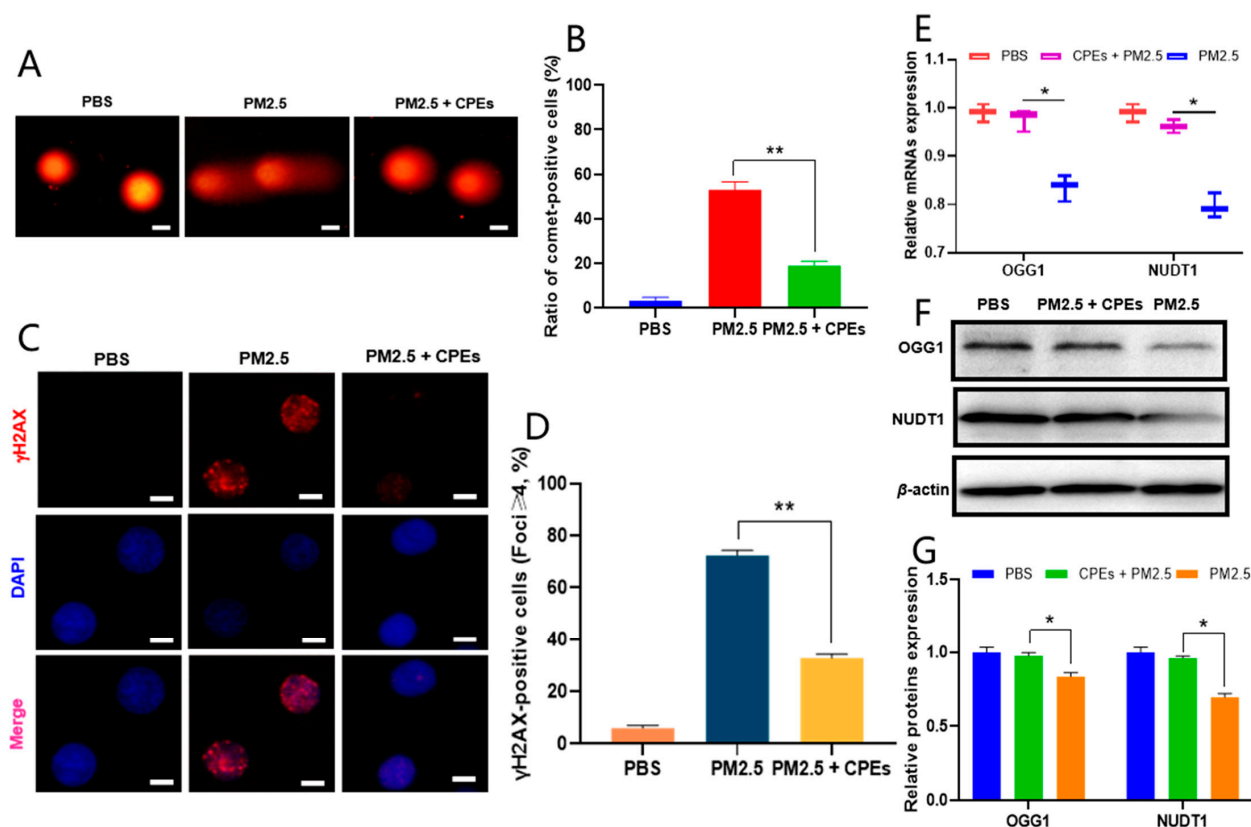


Figure 6. Protective effect of CPEs against genotoxicity induced by PM2.5. Cells were co-treated with CPEs (10 mg mL^{-1}) and PM2.5 ($100 \mu\text{g mL}^{-1}$) for 24 h. (A) Alkaline comet assay detected DNA single-strand damage and representative photographs of comets (scale bar: $10 \mu\text{m}$). (B) Analysis results represented the ratio of comet cells from 200 randomly chosen cells. (C) DNA double-strand breaks were illustrated by γ H2AX foci formation. Anti- γ H2AX monoclonal antibody (red) was used for DNA damage foci immunofluorescence and DAPI (blue) was used for nuclei staining (scale bar: $10 \mu\text{m}$). (D) Percentage of γ H2AX-positive cells of fibroblasts. (E) The relative mRNA expression of *NUDT1* and *OGG1* were normalized to β -actin expression. (F,G) Western blot analysis of *NUDT1* and *OGG1* protein levels with PM2.5 or plus CPE treatment at 24 h and the relative protein expression analysis results. All results are expressed as mean \pm SD of three biological replicates. * $p < 0.05$; ** $p < 0.01$ compared with PM2.5.

3.5. The Protective Effect of CPEs for Hepatotoxicity and Survival of Zebrafish under PM2.5 Exposure

Zebrafish are considered to be an ideal animal model for toxicological evaluation because they are sensitive to changes in their surroundings. The present investigation used larvae of zebrafish to assess PM2.5 hepatotoxicity and the protective effect of CPEs. Normal physiological functions of the liver are characterized by apolipoprotein. Our findings demonstrated that PM2.5 decreased the expression of GFP-labeled apolipoprotein and weakened the fluorescence signal in the liver of zebrafish larvae, implying that PM2.5 adversely influenced the normal physiological function of the liver (Figure 7A). However, with the supplement of CPEs, the PM2.5-induced side effects were significantly alleviated, and the fluorescence signal was restored (Figure 7B).

To investigate the in vivo protective effect of CPEs, we increased PM2.5 extract concentration in the zebrafish culture environment to 10 mg mL^{-1} and examined the differences in zebrafish survival in the presence or absence of CPEs. Zebrafish in the PM2.5 group died in a time-dependent manner (Figure 7C); they started dying after 5 min (average survival rate 64.6%, the same as below), and practically all the zebrafish in the PM2.5 group died after 10 min (down to 23.9%) (Figure 7D). However, in the CPE group, the scavenging

activity of CPEs reduced PM2.5-induced mortality of zebrafish exposure throughout the process (5 min, 96.7%; 10 min, 92.5%) (Figure 7D). These data strongly demonstrate that CPEs can prevent the adverse effects of PM2.5 on the body of zebrafish.

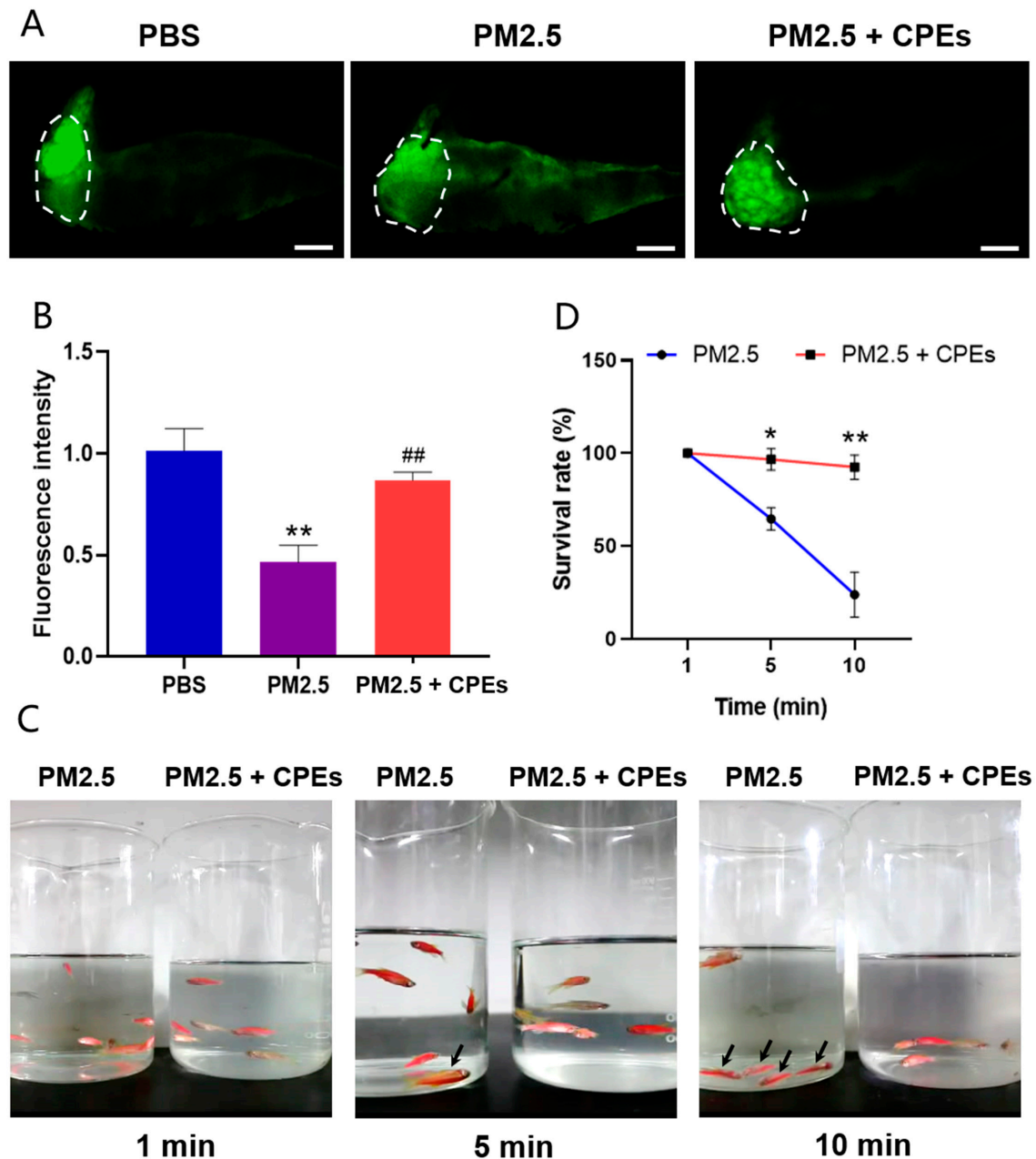


Figure 7. CPE protection effect in Zebrafish hepatotoxicity and survival assay against PM2.5. (A) Viviperception of the larvae tg (Apo14: GFP) liver phenotype by fluorescence microscopic images (green fluorescence and white outline, scale bar: 200 μm). (B) Fluorescence intensity of the liver of larval exposed to PM2.5 ($100 \mu\text{g mL}^{-1}$) under fluorescence microscopy. (C) Video capture of zebrafish survival state after treatment of PM2.5 (10 mg mL^{-1}) or plus CPEs (10 mg mL^{-1}) at 1, 5, 10 min (black arrow refers to dead zebrafishes). (D) The percentage of zebrafish survival rate. All results are expressed as mean \pm SD of three biological replicates. (B) ** $p < 0.01$ compared with PBS, ## $p < 0.01$ compared with PM2.5. (D) * $p < 0.05$, ** $p < 0.01$ compared with PM2.5.

4. Discussion

The bulk of current investigations on the toxicity of atmospheric PM_{2.5} is focused on its impact on respiratory and cardiovascular disorders. Skin, being the first line of defense between the human body and the environment, is directly exposed to PM_{2.5}. Owing to its tiny particle size, PM_{2.5} can directly invade the skin tissues independent of respiratory inhalation. Furthermore, a majority of research focuses solely on the impact of PM_{2.5} on cell or bodily injury. However, little thought has been given to lessening or preventing the adverse effects of PM_{2.5}. In the present work, the cell viability assay demonstrated a gradual decrease in fibroblast viability following an increase in PM_{2.5} concentration. However, the intervention of CPEs significantly restored cell viability at a PM_{2.5} concentration of 100 µg mL⁻¹ (Figure 4A), in this view, we determined 100 µg mL⁻¹ as the effective concentration of PM_{2.5} to reflect its cytotoxicity for subsequent cell experiments. Furthermore, we used the copper ion chelation experiment as a reference to determine whether CPEs could exert biological activity and purify metal ions at a concentration of 10 mg mL⁻¹, which is consistent with previous findings [22]. Therefore, we selected 10 mg mL⁻¹ CPEs extracted using patented technology to block PM_{2.5} cytotoxicity in subsequent cell and animal experiments.

Cell viability, as a fundamental biological feature of cells, maintains the basic survival state of cells and influences the cell cycle and cell proliferation. PM_{2.5} and CPEs were employed as intervention variables to detect the cell viability of human skin fibroblasts based on the evaluated working concentration. The present investigation revealed that PM_{2.5} significantly decreased the cell viability and proliferation rate of human skin fibroblasts in a concentration- and time-dependent manner. However, the addition of CPEs effectively alleviated the decrease in cell viability caused by PM_{2.5}, demonstrating that CPEs antagonized PM_{2.5} and reduced its negative effect.

Decreased mitochondrial function could further impair the cell cycle and cell proliferation. Moreover, it has been reported that CPEs can promote proliferation and progression of the cell cycle [29]. In this study, PM_{2.5} interrupted the normal cell cycle and caused S-phase arrest. Results of EdU staining and flow cytometry showed that PM_{2.5} treatment increased the proportion of cells in the G₀/G₁ phase and decreased the number of cells in the S-phase. Notably, CPE treatment dampened the effects of PM_{2.5} on the cell cycle of fibroblasts, and the proportion of cells in the S-phase was nearly similar to that in the control group. Meanwhile, we found that CPEs maintained a normal cell number as revealed by the cell count results. These findings demonstrated that CPEs resisted the cytotoxicity induced by PM_{2.5} and alleviated the suppression of cell viability, cell cycle arrest, and reduced proliferation capacity following PM_{2.5} exposure.

Genomic integrity is the structural basis of the normal physiological activities of individual cells. It has been reported that polycyclic aromatic hydrocarbons (PAHs) in PM_{2.5} induce chromosome structural fracture and DNA damage, thereby causing physiological dysfunction, apoptosis and senescence [30]. The comet assay and γH2AX foci staining assays are the typical methods used to detect DNA integrity and to evaluate the genotoxicity induced by PM_{2.5}. In this study, the comet assay parameters including the tail DNA, tail length, tail moment and number of γH2AX-positive foci were significantly increased after PM_{2.5} treatment, suggesting that PM_{2.5} caused considerable damage to both single and double strands of DNA as shown in Figure 5A, C. CPE intervention significantly reduced the DNA damage caused by PM_{2.5}. Due to the complexity of PM_{2.5} components, the potential DNA damage repair mechanism of CPEs involves the reduction of intermediate metabolite 8-oxo-dGTP by BER-related hydrolases *NUDT1* and *OGG1*, hydrolysis of 8-oxoG modification on the DNA double-strand, and reduction in the accumulation of 8-oxoG, potentially affecting DNA instability [31]. Our results reveal that PM_{2.5} inhibited the nucleic acid and protein expression of related hydrolases following DNA damage, thus aggravating the DNA damage. However, CPEs restored the nucleic acid and protein levels of hydrolases, suggesting that CPEs may repair DNA damage by increasing gene expression and by restoring enzyme activity. However, the specific molecular mechanism

by which CPEs alleviate PM2.5-induced DNA damage and suppression of DNA repair-related hydrolases still needs to be further studied. Our results indicate that CPEs stabilized the structural integrity of the genome, alleviated DNA damage induced by PM2.5, and improved DNA repair functions by restoring the normal expression of repair genes at mRNA and protein levels.

As an ideal animal model for toxicological evaluation [32,33], zebrafish exhibit high sensitivity to PM2.5. The liver toxicology test revealed that PM2.5 inhibited apolipoprotein synthesis, which affected the normal physiological function of zebrafish liver. In vivo survival experiments showed that high concentrations of PM2.5 directly impaired the living conditions of zebrafish and caused death. However, CPEs alleviated hepatotoxicity and improved the survival rate of zebrafish. Therefore, it is expected to become a functional food that can prevent hepatotoxicity.

Chlorella has been widely used as a nutritional supplement in the production of health products and food additives, and its extract CPE has been shown to have a variety of positive regulatory biological functions. Our study has shown that CPE has good antagonistic and repairing effects on cellular and organismal damage caused by PM2.5. *Chlorella vulgaris* has been reported to have a purifying effect on heavy metal pollution in water [34] and has a better epi-modifying effect on polycyclic aromatic hydrocarbon (PAH) compounds in PM2.5 [35], reducing the overall methylation level of cells under the effect of PAHs and reducing the level of PAH metabolites, thus reducing the risk of cancer development. Combined with our results, it is possible to use CPEs as raw material for the development and application of PM2.5-related purification products, such as the addition of CPE in indoor air purifiers, or the development of anti-haze masks with CPE add-ons. However, the selection of CPE dosage forms in different products still needs further research and demonstration. In terms of mechanism, our experiments confirmed that CPE has the characteristics of heavy metal chelation and can purify pollutants in water, suggesting that CPE has certain characteristics of physical adsorption. The cell experiment further proved that CPE can promote the recovery of normal physiological function of cells, stabilize the genomic structure of DNA, reduce genotoxicity, and further reduce the toxicity of PM2.5. It is inferred that CPE may play different regulatory functions in regulating the cell cycle and maintaining proliferation pathways and epigenetic modification, which will be the main research direction of our follow-up work and which need further research and exploration.

5. Conclusions

In summary, we successfully extracted the *Chlorella*-active ingredient, *Chlorella* purification effector molecules (CPEs), through our self-designed patented technology and proved that it had strong biological activity. We employed another patented technology to collect PM2.5 from the atmosphere. The results demonstrated that CPEs reduced several adverse effects caused by PM2.5 exposure in human skin fibroblasts, such as cytotoxicity, cell cycle arrest, decreased proliferation ability, and significant decline in cell numbers. At the molecular level, CPEs mitigated cell DNA damage caused by PM2.5, stabilized the integrity of the genome structure, and alleviated PM2.5-induced genotoxicity. In addition, we found that downregulation of *NUDT1* and *OGG1* by PM2.5 disrupted the normal DNA repair systems, but CPE treatment restored this effect. CPEs significantly reduced the hepatotoxicity and mortality of zebrafish following PM2.5 exposure. Our study provides a theoretical basis for further studies on the bioactivity and mechanisms of CPEs against the effects of PM2.5. The present results support the wider application of CPEs in the cosmetics and health industries.

Supplementary Materials: The following supporting information can be downloaded at: <https://www.mdpi.com/article/10.3390/cosmetics10020063/s1>, Video S1: Zebrafish toxicity and protection testing.

Author Contributions: X.W.: conceived the study, designed the methodology, conducted data analysis and experiments, wrote the original draft of the manuscript; X.L.: performed experiments, obtained experimental resources; X.J.: obtained experimental resources; F.X.: performed experiments, performed validation tests; Y.L.: performed experiments, obtained experimental resources; G.X.: conceived the study, supervised the project, revised and edited the manuscript, acquired funds. All authors have read and agreed to the published version of the manuscript.

Funding: This research received no external funding.

Institutional Review Board Statement: The experiment was performed in three independent replicates. All experiments complied with guidelines for the Animal Care Committee of East China University of Science and Technology (approval number #2006272).

Informed Consent Statement: Not applicable.

Data Availability Statement: The data are contained within the article and Supplementary Materials.

Acknowledgments: This work was supported by Shanghai Jiayu Bio-technology Co., Ltd for raw material and extraction technical support. We would like to express cordial gratitude to Ugel Cosmetics Pte. Ltd., Bo Li Xi Biotechnology Co., Ltd., for their remarkable technical guidance.

Conflicts of Interest: The authors declare no conflict of interest.

References

1. Fernando, P.; Piao, M.J.; Zhen, A.X.; Ahn, M.J.; Yi, J.M.; Choi, Y.H.; Hyun, J.W. Extract of *Cornus officinalis* Protects Keratinocytes from Particulate Matter-induced Oxidative Stress. *Int. J. Med. Sci.* **2020**, *17*, 63–70. [[CrossRef](#)] [[PubMed](#)]
2. Hyun, S.W.; Kim, J.; Park, B.; Jo, K.; Lee, T.G.; Kim, J.S.; Kim, C.S. Apricot Kernel Extract and Amygdalin Inhibit Urban Particulate Matter-Induced Keratoconjunctivitis Sicca. *Molecules* **2019**, *24*, 650. [[CrossRef](#)] [[PubMed](#)]
3. Lee, J.H.; Kim, H.J.; Jee, Y.; Jeon, Y.J.; Kim, H.J. Antioxidant potential of *Sargassum horneri* extract against urban particulate matter-induced oxidation. *Food Sci. Biotechnol.* **2020**, *29*, 855–865. [[CrossRef](#)] [[PubMed](#)]
4. Lee, T.G.; Hyun, S.W.; Jo, K.; Park, B.; Lee, I.S.; Song, S.J.; Kim, C.S. *Achyranthis radix* Extract Improves Urban Particulate Matter-Induced Dry Eye Disease. *Int. J. Environ. Res. Public Health* **2019**, *16*, 3229. [[CrossRef](#)] [[PubMed](#)]
5. Lee, W.; Jeong, S.Y.; Gu, M.J.; Lim, J.S.; Park, E.K.; Baek, M.C.; Kim, J.S.; Hahn, D.; Bae, J.S. Inhibitory effects of compounds isolated from *Dioscorea batatas* Decne peel on particulate matter-induced pulmonary injury in mice. *J. Toxicol. Environ. Health. Part A* **2019**, *82*, 727–740. [[CrossRef](#)]
6. Lee, Y.Y.; Yang, W.K.; Han, J.E.; Kwak, D.; Kim, T.H.; Saba, E.; Kim, S.D.; Lee, Y.C.; Kim, J.S.; Kim, S.H.; et al. *Hypericum ascyron* L. extract reduces particulate matter-induced airway inflammation in mice. *Phytother. Res. PTR* **2021**, *35*, 1621–1633. [[CrossRef](#)]
7. Moon, J.Y.; Ngoc, L.T.N.; Chae, M.; Tran, V.V.; Lee, Y.C. Effects of Microwave-Assisted *Opuntia Humifusa* Extract in Inhibiting the Impacts of Particulate Matter on Human Keratinocyte Skin Cell. *Antioxidants* **2020**, *9*, 271. [[CrossRef](#)]
8. Safi, C.; Zebib, B.; Merah, O.; Pontalier, P.-Y.; Vaca-Garcia, C. Morphology, composition, production, processing and applications of *Chlorella vulgaris*: A review. *Renew. Sustain. Energy Rev.* **2014**, *35*, 265–278. [[CrossRef](#)]
9. Ramos-Romero, S.; Torrella, J.R.; Pagès, T.; Viscor, G.; Torres, J.L. Edible Microalgae and Their Bioactive Compounds in the Prevention and Treatment of Metabolic Alterations. *Nutrients* **2021**, *13*, 563. [[CrossRef](#)]
10. Zakaria, S.M.; Kamal, S.M.M.; Harun, M.R.; Omar, R.; Siajam, S.I. Subcritical Water Technology for Extraction of Phenolic Compounds from *Chlorella* sp. Microalgae and Assessment on Its Antioxidant Activity. *Molecules* **2017**, *22*, 1105. [[CrossRef](#)]
11. Ishiguro, S.; Robben, N.; Burghart, R.; Cote, P.; Greenway, S.; Thakkar, R.; Upreti, D.; Nakashima, A.; Suzuki, K.; Comer, J.; et al. Cell Wall Membrane Fraction of *Chlorella sorokiniana* Enhances Host Antitumor Immunity and Inhibits Colon Carcinoma Growth in Mice. *Integr. Cancer Ther.* **2020**, *19*, 1534735419900555. [[CrossRef](#)] [[PubMed](#)]
12. Horii, N.; Hasegawa, N.; Fujie, S.; Uchida, M.; Iemitsu, K.; Inoue, K.; Iemitsu, M. Effect of combination of *Chlorella* intake and aerobic exercise training on glycemic control in type 2 diabetic rats. *Nutrition* **2019**, *63–64*, 45–50. [[CrossRef](#)] [[PubMed](#)]
13. Hamouda, R.A.; Abd El Latif, A.; Elkaw, E.M.; Alotaibi, A.S.; Alenzi, A.M.; Hamza, H.A. Assessment of Antioxidant and Anticancer Activities of Microgreen Alga *Chlorella vulgaris* and Its Blend with Different Vitamins. *Molecules* **2022**, *27*, 1602. [[CrossRef](#)] [[PubMed](#)]
14. Napolitano, G.; Fasciolo, G.; Salbitani, G.; Venditti, P. *Chlorella sorokiniana* Dietary Supplementation Increases Antioxidant Capacities and Reduces Ros Release in Mitochondria of Hyperthyroid Rat Liver. *Antioxidants* **2020**, *9*, 883. [[CrossRef](#)]
15. Orona, N.S.; Astort, F.; Maglione, G.A.; Ferraro, S.A.; Martin, M.; Morales, C.; Mandalunis, P.M.; Brites, F.; Tasat, D.R. Hazardous effects of urban air particulate matter acute exposure on lung and extrapulmonary organs in mice. *Ecotoxicol. Environ. Saf.* **2020**, *190*, 110120. [[CrossRef](#)]

16. Senthil Kumar, S.; Muthuselvam, P.; Pugalenti, V.; Subramanian, N.; Ramkumar, K.M.; Suresh, T.; Suzuki, T.; Rajaguru, P. Toxicoproteomic analysis of human lung epithelial cells exposed to steel industry ambient particulate matter (PM) reveals possible mechanism of PM related carcinogenesis. *Environ. Pollut.* **2018**, *239*, 483–492. [[CrossRef](#)]
17. Woodward, N.C.; Pakbin, P.; Saffari, A.; Shirmohammadi, F.; Haghani, A.; Sioutas, C.; Cacciottolo, M.; Morgan, T.E.; Finch, C.E. Traffic-related air pollution impact on mouse brain accelerates myelin and neuritic aging changes with specificity for CA1 neurons. *Neurobiol. Aging* **2017**, *53*, 48–58. [[CrossRef](#)]
18. Ibrionke, O.; Carranza, C.; Sarkar, S.; Torres, M.; Choi, H.T.; Nwoko, J.; Black, K.; Quintana-Belmares, R.; Osornio-Vargas, Á.; Ohman-Strickland, P.; et al. Urban Air Pollution Particulates Suppress Human T-Cell Responses to Mycobacterium Tuberculosis. *Int. J. Environ. Res. Public Health* **2019**, *16*, 4112. [[CrossRef](#)]
19. Guanggang, X. Anti-Pollution Testing Device and Method. CN106442250B, 3 July 2020.
20. Guanggang, X. Preparation of Chlorella Deep Purification Factor. CN106236623A, 21 December 2016.
21. Liang, P.; Xing, X.; Wu, J.; Song, J.; Liu, Q. PM2.5 promotes apoptosis of human epidermal melanocytes through promoting oxidative damage and autophagy. *Gen. Physiol. Biophys.* **2020**, *39*, 569–577. [[CrossRef](#)]
22. Zhuang, X.; Zhang, D.; Qin, W.; Deng, J.; Shan, H.; Tao, L.; Li, Y. A comparison on the preparation of hot water extracts from Chlorella pyrenoidosa (CPEs) and radical scavenging and macrophage activation effects of CPEs. *Food Funct.* **2014**, *5*, 3252–3260. [[CrossRef](#)]
23. Zheng, F.; Tang, Q.; Wu, J.; Zhao, S.; Liang, Z.; Li, L.; Wu, W.; Hann, S. p38 α MAPK-mediated induction and interaction of FOXO3a and p53 contribute to the inhibited-growth and induced-apoptosis of human lung adenocarcinoma cells by berberine. *J. Exp. Clin. Cancer Res.* **2014**, *33*, 36. [[CrossRef](#)] [[PubMed](#)]
24. Li, B.; Hu, X.; Yang, Y.; Zhu, M.; Zhang, J.; Wang, Y.; Pei, X.; Zhou, H.; Wu, J. GAS5/miR-21 Axis as a Potential Target to Rescue ZCL-082-Induced Autophagy of Female Germline Stem Cells In Vitro. *Mol. Ther. Nucleic Acids* **2019**, *17*, 436–447. [[CrossRef](#)] [[PubMed](#)]
25. Xiang, G.; Li, D.; Yuan, J.; Guan, J.; Zhai, H.; Shi, M.; Tao, L. Carbamate insecticide methomyl confers cytotoxicity through DNA damage induction. *Food Chem. Toxicol.* **2013**, *53*, 352–358. [[CrossRef](#)]
26. Zhu, Y.; Ma, N.; Li, H.X.; Tian, L.; Ba, Y.F.; Hao, B. Berberine induces apoptosis and DNA damage in MG63 human osteosarcoma cells. *Mol. Med. Rep.* **2014**, *10*, 1734–1738. [[CrossRef](#)] [[PubMed](#)]
27. Sokolov, M.V.; Smilenov, L.B.; Hall, E.J.; Panyutin, I.G.; Bonner, W.M.; Sedelnikova, O.A. Ionizing radiation induces DNA double-strand breaks in bystander primary human fibroblasts. *Oncogene* **2005**, *24*, 7257–7265. [[CrossRef](#)] [[PubMed](#)]
28. Tian, M.; Liu, W.; You, H.; Zhao, Q.; Ouyang, L.; Gao, B.; Zhang, X.; Che, N. Protective effect of Yiguanjian decoction against DNA damage on concanavalin A-induced liver injury mice model. *J. Tradit. Chin. Med.* **2016**, *36*, 471–478. [[CrossRef](#)] [[PubMed](#)]
29. Okamoto, Y.; Haraguchi, Y.; Yoshida, A.; Takahashi, H.; Yamanaka, K.; Sawamura, N.; Asahi, T.; Shimizu, T. Proliferation and differentiation of primary bovine myoblasts using Chlorella vulgaris extract for sustainable production of cultured meat. *Biotechnol. Prog.* **2022**, *38*, e3239. [[CrossRef](#)]
30. Abbas, I.; Badran, G.; Verdin, A.; Ledoux, F.; Roumie, M.; Guidice, J.-M.L.; Courcot, D.; Garçon, G. In vitro evaluation of organic extractable matter from ambient PM2.5 using human bronchial epithelial BEAS-2B cells: Cytotoxicity, oxidative stress, pro-inflammatory response, genotoxicity, and cell cycle deregulation. *Environ. Res.* **2019**, *171*, 510–522. [[CrossRef](#)]
31. Schmaltz, L.F.; Cenicerros, J.E.; Lee, S. Structure of the major oxidative damage 7,8-dihydro-8-oxoguanine presented into a catalytically competent DNA glycosylase. *Biochem. J.* **2022**, *479*, 2297–2309. [[CrossRef](#)]
32. Bai, Z.; Jia, K.; Chen, G.; Liao, X.; Cao, Z.; Zhao, Y.; Zhang, C.; Lu, H. Carbamazepine induces hepatotoxicity in zebrafish by inhibition of the Wnt/ β -catenin signaling pathway. *Environ. Pollut.* **2021**, *276*, 116688. [[CrossRef](#)]
33. Cheng, Y.C.; Wu, T.S.; Huang, Y.T.; Chang, Y.; Yang, J.J.; Yu, F.Y.; Liu, B.H. Aflatoxin B1 interferes with embryonic liver development: Involvement of p53 signaling and apoptosis in zebrafish. *Toxicology* **2021**, *458*, 152844. [[CrossRef](#)] [[PubMed](#)]
34. Ahmed, A.; Jyothi, N.; Ramesh, A. Improved ammonium removal from industrial wastewater through systematic adaptation of wild type Chlorella pyrenoidosa. *Water Sci. Technol.* **2017**, *75*, 182–188. [[CrossRef](#)] [[PubMed](#)]
35. Yang, M.; Youn, J.I.; Kim, S.J.; Park, J.Y. Epigenetic modulation of Chlorella (Chlorella vulgaris) on exposure to polycyclic aromatic hydrocarbons. *Environ. Toxicol. Pharmacol.* **2015**, *40*, 758–763. [[CrossRef](#)] [[PubMed](#)]

Disclaimer/Publisher’s Note: The statements, opinions and data contained in all publications are solely those of the individual author(s) and contributor(s) and not of MDPI and/or the editor(s). MDPI and/or the editor(s) disclaim responsibility for any injury to people or property resulting from any ideas, methods, instructions or products referred to in the content.